MCB
Journals.ASM.org

Histone Methylation Has Dynamics Distinct from Those of Histone Acetylation in Cell Cycle Reentry from Quiescence

Philipp Mews,[a,b] Barry M. Zee,[a,c] Sherry Liu,[a,c] Greg Donahue,[a,b] Benjamin A. Garcia,[a,c] Shelley L. Berger[a,b,c]

Penn Epigenetics Program,[a] Department of Cell and Developmental Biology,[b] and Department of Biochemistry and Biophysics,[c] Perelman School of Medicine at the University of Pennsylvania, Philadelphia, Pennsylvania, USA

Cell growth is attuned to nutrient availability to sustain homeostatic biosynthetic processes. In unfavorable environments, cells enter a nonproliferative state termed quiescence but rapidly return to the cell cycle once conditions support energetic needs. Changing cellular metabolite pools are proposed to directly alter the epigenome via histone acetylation. Here we studied the relationship between histone modification dynamics and the dramatic transcriptional changes that occur during nutrient-induced cell cycle reentry from quiescence in the yeast *Saccharomyces cerevisiae*. SILAC (stable isotope labeling by amino acids in cell culture)-based mass spectrometry showed that histone methylation—in contrast to histone acetylation—is surprisingly static during quiescence exit. Chromatin immunoprecipitation followed by massive parallel sequencing (ChIP-seq) revealed genome-wide shifts in histone acetylation at growth and stress genes as cells exit quiescence and transcription dramatically changes. Strikingly, however, the patterns of histone methylation remain intact. We conclude that the functions of histone methylation and acetylation are remarkably distinct during quiescence exit: acetylation rapidly responds to metabolic state, while methylation is independent. Thus, the initial burst of growth gene reactivation emerging from quiescence involves dramatic increases of histone acetylation but not of histone methylation.

Cells constantly sense and integrate environmental cues to control proliferative growth, but the underlying molecular mechanisms remain unclear. Eukaryotic cells, including adult stem cells, typically exist in a state of growth arrest—quiescence—that is distinguished by two principal qualities: quiescent cells both safeguard cell identity and retain the ability to resume proliferation once external cues become favorable (1–3). Remarkably little is known about the molecular processes that mediate quiescence exit and the transition to proliferative growth, which requires massive changes in cell metabolism and reprogramming of global gene expression (4–6).

Recent evidence suggests that the metabolic state is a principle regulator of quiescence establishment and exit via epigenetic changes that alter gene expression (7–9). A clear example is that nutrient-induced increases in acetyl coenzyme A (acetyl-CoA) pools promote chromatin acetylation and growth gene transcription (10, 11). Rhythmic fluctuations of acetyl-CoA levels are characteristic of the metabolic cycle that budding yeast cells enter during growth under nutrient-limiting conditions. In such a milieu, recurrent bursts of acetyl-CoA production by the acetyl-CoA synthase Acs2p have been linked to increased histone acetylation and growth gene expression, indicating a functional connection between metabolic state and gene transcription via chromatin acetylation (10). Indeed, studies in both the yeast *Saccharomyces cerevisiae* and activated lymphocytes indicate that glucose-induced histone acetylation is a critical and highly conserved driver of quiescence exit (11–13). In mammalian cells, acetyl-CoA synthesis by ATP-citrate lyase (ACL) has been shown to link nutrient-dependent histone acetylation and cellular growth. These findings suggest a model of transcriptional control via conserved connections between metabolic and epigenetic states (14–16).

Even though metabolic activities are coupled to histone acetylation and growth gene transcription, it is uncertain whether cellular metabolites also influence histone methylation to dynamically regulate transcription. Notably, histone methylation is a far more complex process than acetylation. Histone methyltransferase (HMT) and histone demethylase (HDM) enzymes regulate mono-, di-, and trimethylation states of multiple histone lysine residues that have diverse functions in transcriptional control (17). Histone methylation is dependent on the central metabolite *S*-adenosyl methionine (SAM). Based on this, it has been speculated that intracellular SAM concentrations may modulate chromatin structure in response to the metabolic milieu (18). The high-energy methyl donor SAM is generated from methionine by methionine adenosyltransferase (MAT) enzymes in an ATP-consuming reaction, and its chromatin-localized synthesis concentration is believed to fine-tune histone methylation (19). Recent evidence suggests that threonine metabolism may selectively influence di- and trimethylation of histone H3 lysine 4 (H3K4me3) specifically in mouse embryonic stem cells (mESCs) by supplying acetyl-CoA for SAM synthesis during mESC colony growth (20).

Overall, it remains unknown whether histone methylation is a broad energy-sensing modification that adapts transcription relative to the metabolic state, akin to histone acetylation. The dynamics of histone methylation have not been examined in cells transitioning from minimal to high metabolic activity, and methods to reliably determine residue-specific methylation dynamics using mass spectrometry have only recently been developed (21). To explore the role of histone methylation as a putative energy sensor in the context of massive metabolic and transcriptional

Received 6 June 2014 Returned for modification 14 July 2014
Accepted 14 August 2014
Published ahead of print 25 August 2014
Address correspondence to Shelley L. Berger, bergers@mail.med.upenn.edu.

doi:10.1128/MCB.00763-14

reprogramming, we investigated the temporal dynamics of global histone methylation during cell cycle reentry of the quiescent budding yeast *S. cerevisiae*. Our results show that histone methylation operates in stark contrast to highly dynamic glucose-induced histone acetylation, with methylation levels remaining highly stable during quiescence exit.

MATERIALS AND METHODS

Quiescence establishment and exit protocol. Western blotting, stable isotope labeling by amino acids in cell culture (SILAC), RNA sequencing (RNA-seq), and chromatin immunoprecipitation followed by massive parallel sequencing (ChIP-seq) experiments were performed in BY4741 (*MAT***a** *his3*Δ*1 leu2*Δ*0 met15*Δ*0 ura3*Δ*0*; Invitrogen). To establish quiescence, yeast cells were cultured in 2% synthetic complete medium (SCM; 2% glucose–0.5% ammonium sulfate–0.2% SCM supplement [Bufferad]–0.17% yeast nitrogen base [Bufferad]) for 72 h before their transfer into water for complete nutrient starvation and quiescence establishment at 30°C, ensuring a homogenous nondividing cell population, as previously described (22). Quiescence exit was induced on day 8 by resuspending pelleted quiescent cells into fresh 30°C-prewarmed 2% SC medium at an optical density at 600 nm (OD_{600}) of 0.4. At various time points, culture aliquots were taken, and cells were harvested by centrifugation or microfiltration and stored at −80°C for subsequent analyses as outlined below.

Yeast whole-cell extract preparation and Western blotting. Yeast cells were harvested by centrifugation at 4,000 rpm for 4 min at 4°C. Cells were washed with ice-cold water once and broken in 50 mM Tris-HCl (pH 7.4)–300 mM NaCl–0.5% NP-40–10% glycerol–1 mM EDTA (pH 8)–protease inhibitor cocktail (Complete; Roche) using silica beads and a bead beater (Bio-Spec). The lysate was sonicated (Bioruptor; Diagenode) for 5 min and cleared by centrifugation at 14,000 rpm at 4°C for 15 min. The supernatant was collected and stored at −80°C. Protein estimation was determined using Bradford dye. Extracts were resolved on SDS-polyacrylamide gels, Western blotting performed by standard methods, and images of the Western blots were taken with a Fujifilm LAS-4000 imager.

Antibodies. The primary antibodies used were anti-H3 (1:1,000; Abcam no. ab1791), anti-H3K9ac (1:1,000; Active Motif no. 39137), anti-H3K4me1 (1:500; Abcam no. ab8895), H3K4me2 (1:1,000; Active Motif no. 39141), anti-H3K4me3 (1:1,000; Abcam no. ab8580), anti-H3K36me1 (1:1,000; Abcam no. ab9048), anti-H3K36me3 (1:1,000; Active Motif no. 61101), anti-H3K79me3 (1:1,000; Abcam no. ab2621), anti-H4K5ac (1:1,000; Millipore no. 07-327), and anti-H4K8ac (1:1,000; Millipore no. 07-328).

Cell culture and SILAC. For the methyl-SILAC and lysine SILAC time course experiments, quiescent cell cultures were pelleted at 4,000 rpm for 3 min at 30°C and resuspended with 2% SC medium that was depleted of unlabeled methionine or lysine (SC dropout mixtures; Sunrise Science Products) and supplemented with equimolar amounts of L-methionine-methyl-[^{13}C]D_3 (Sigma-Aldrich) or [$^{13}C_6$, $^{15}N_2$]-lysine (Cambridge Isotope Laboratories), respectively. In order to assess histone acetylation turnover by heavy glucose SILAC, quiescent cells were resuspended in SC medium supplemented with 2% isotopically heavy [$^{13}C_6$]glucose (Sigma-Aldrich). Aliquots were taken at various time points, and cells collected by centrifugation at 4,000 rpm for 3 min, flash frozen, and stored at −80°C for the subsequent nucleus preparation and histone protein purification as outlined below.

Purification of histone proteins for mass spectrometry. Preparation of nuclei was based on published methods (23, 24). In brief, 10^{10} cells were washed in 1 M sorbitol–50 mM potassium phosphate (pH 6.8)–14 mM β-mercaptoethanol at 30°C. In order to achieve complete digestion of the cell wall, cells were resuspended in the same buffer supplemented with Zymolyase 100T (0.4 mg/ml) at 30°C for 30 min to 1.5 h. The digestion was monitored by adding 1% SDS to 20 μl of the digestion reaction mixture and considered complete once the OD_{600} dropped by 95%. Spheroplasted cells were washed in 1 M sorbitol, and cell lysis was achieved in 18% Ficoll–20 mM potassium phosphate (pH 6.8)–1.0 mM $MgCl_2$–0.5 mM EDTA–100 mM sodium butyrate–protease inhibitor cocktail (Complete; Roche) by 60 strokes of a Wheaton Dounce homogenizer on ice. Nuclei were collected after centrifugation at 4,000 rpm from the supernatant and pelleted by ultracentrifugation at 50,000 × *g* for 30 min at 4°C. Pelleted nuclei were resuspended in 0.34 M sucrose–20 mM Tris-HCl (pH 7.4)–50 mM KCl–5.0 mM $MgCl_2$ and purified by ultracentrifugation on a 2 M sucrose cushion at 30,000 × *g* for 30 min at 4°C. Acid extraction to enrich for basic histone proteins was achieved by resuspending nuclei in 10 mM Tris-HCl (pH 8.0)–400 mM NaCl–100 mM sodium butyrate after three washes in 10 mM Tris-HCl (pH 8.0)–0.5% NP-40–75 mM NaCl–100 mM sodium butyrate, and protein precipitation by addition of 20% trichloroacetic acid (TCA), followed by centrifugation, and two washes in acetone–0.1% HCl and acetone alone. The pellet was briefly dried, and proteins were resuspended in water for derivatization.

Histone sample preparation for mass spectrometry. Purified histones were derivatized with propionic anhydride and digested with sequencing-grade trypsin as described before (21, 25). Due to the relative hydrophilicity of the H3 3-8 peptide spanning H3K4 and thus reduced retention and resolution using reversed-phase liquid chromatography (our unpublished data), aliquots from the same histone protein sample were derivatized with benzoic anhydride rather than propionic anhydride. After derivatization with either reagent, both sample preparations were separately diluted in 0.1% acetic acid for desalting before mass-spectrometric (MS) analysis using homemade C_{18} stage tips as previously described (25).

Mass spectrometry analysis and peptide quantification. Histone peptides were loaded by an Eksigent AS2 autosampler onto silica capillary C_{18} columns and resolved by an Agilent 1200 binary high-performance liquid chromatography (HPLC) system as previously reported (21). Peptides were electrosprayed into a linear quadrupole ion trap-Orbitrap mass spectrometer. All MS and MS/MS spectra were analyzed with Qual Browser (version 2.0.7; Thermo Scientific), and peptide abundances were obtained by peak integration of the extracted ion chromatograms as previously described (21).

SAM labeling assay and SAM fluorometry quantification. Cells were harvested by filtration, and selected reaction monitoring (SRM) analysis by mass spectrometry was performed as described by Bajad et al. and Zee et al. (26, 27). To quantify SAM levels, the Bridge-It SAM fluorescence assay (Mediomics) was used according to the manufacturer's instructions.

RNA preparation and RNA-seq. RNA was purified using the Dynabeads mRNA Direct kit (61011; Ambion, Life Technologies) according to the manufacturer's instructions. RNA-seq libraries were prepared using the ScriptSeq v2 RNA-Seq library preparation kit (SSV21124; Epicentre) according to the manufacturer's recommendations, and sequencing was performed on the Illumina Hi-Seq (50-bp single-end reads) platform. RNA-seq data were aligned using the software TopHat (28), and gene expression levels and differences were calculated using Cuffdiff (29). Reads per million reads sequenced per kilobase of exons in the transcript (RPKM) values for exit and log-phase samples were normalized to quiescence scores, log transformed, and visualized using the Partek Genomics Suite (Partek Incorporated).

ChIP-seq. Approximately 50 OD_{600} units of cells were cross-linked in 1% formaldehyde for 10 min at 25°C, quenched by the addition of glycine to 125 mM for 5 min at 25°C, and washed with water. Cells were resuspended in FA lysis buffer (50 mM HEPES [pH 7.5]–150 mM NaCl–2 mM EDTA–1% Triton X-100–0.2% SDS–Mini EDTA-free protease inhibitor cocktail tablets [Complete; Roche]). One milliliter of silica beads was added to each tube, and cells were disrupted twice for 3 min each for the LOG sample and four times for 3 min each for the cells in the quiescent state (Q), early-exiting cells before DNA replication (E30), and late-exiting cells after the start of DNA replication (E240) at maximum speed with intermediate incubation at −20°C for 3 min (mini-Beadbeater 96; Biospec). Chromatin was washed twice with FA lysis buffer and sonicated for 30 cycles (30 s on at high level and 30 s off per cycle) (Bioruptor; Diagenode). Cellular debris was removed by centrifugation at 14,000 rpm for

15 min at 4°C. ChIP was performed as previously described (30); ChIP using H3K9ac and H4K12ac antibodies for quiescence extracts were completed with 5-fold the input used for all other ChIP experiments. For each ChIP assay, 30 μl of protein G-Dynabeads (100.02D; Invitrogen) was prepared using 5 μg of antibody. Controls with IgG and no antibody were routinely performed. The ChIP DNA was used to make sequencing libraries using standard Illumina library single-end construction procedures. Sequencing was performed on the Illumina Hi-Seq (50-bp single-end reads) platform.

Sequencing analysis. ChIP-seq reads were aligned to the sacCer2 assembly of the *S. cerevisiae* genome using the Bowtie alignment software (31). For growth and stress gene box plot analysis, each gene of the respective group was assigned a score by computing the area under the curve (AUC) of the ChIP-seq signal over the gene body (H3K36me3) or within 250 bp of the transcription start site (TSS±250bp) (H3K4me3, H3K9ac, and H3K12ac). Scores for a given locus in a given state were computed by normalizing the number of tags aligned to the locus by the total number of bases sequenced per barcoded sample as well as by total histone and locus length. Box plots were generated in R. Yeast TSS and open reading frame (ORF) locations were obtained by querying the Ensembl database (www.ensembl.org).

Gene ontology and Venn diagrams. Gene ontology (GO) analysis was performed using DAVID (http://david.abcc.ncifcrf.gov/). The GO terms were clustered using the tool VENNY (http://bioinfogp.cnb.csic.es/tools/venny/), and Euler diagrams were generated using the EulerAPE drawing tool (http://www.eulerdiagrams.org/eulerAPE/) and were subsequently edited for color in PowerPoint 2010 (Microsoft).

RESULTS

Histone methylation does not change globally during reentry into the cell cycle. Nutrient abundance induces quiescence exit and stimulates vast changes in cellular metabolism. Presently, the metabolic state is under intense investigation as a principal regulator of both chromatin and gene expression (8). Indeed, previous observations showed that global histone acetylation is dramatically altered during nutrient starvation and refeeding (11). During nutrient-induced quiescence exit, glycolytic metabolism has been found to be the central driver of bursts of histone acetylation (11). We investigated the unexplored changes in histone methylation that may occur upon quiescence establishment and during cell cycle reentry.

Quiescence establishment in yeast is a gradual process involving the stepwise acquisition of various quiescence traits, culminating in the final cessation of proliferation. In order to obtain a homogenous population of quiescent cells and eliminate contamination of slowly cycling subpopulations, we achieved quiescence, as previously described (22), by transferring cells from carbon-exhausted medium into water to ensure complete nutrient starvation prior to the induction of quiescence exit. To investigate and compare chromatin modification dynamics over the course of this process, we examined proliferating cells (LOG), cells in the quiescent state (Q), early-exiting cells before DNA replication (E30), and late-exiting cells after DNA replication commenced (E240) (Fig. 1A). We measured changes in global histone methylation abundance by Western blotting and stable isotope labeling by amino acids in cell culture (SILAC)-mass spectrometry (referred to here as SILAC). We then used chromatin immunoprecipitation followed by massive parallel sequencing (ChIP-seq) to examine changes in local genic modification patterns. In each of these experimental approaches, we compared histone methylation to histone acetylation, which is known to undergo dramatic fluctuations in cell cycle exit and reentry.

First, to confirm that quiescence exit results in the expected dramatic gene expression changes in our experiments, we performed RNA sequencing. As previously noted by gene expression microarray analysis (4–6), we observed that during exit from quiescence, nutrients trigger a massive transcriptional response that involves one third of yeast genes. The rapid transformation of the global gene expression program produces an mRNA transcriptome in the early exit (E30) that closely resembles the transcriptional profile of cycling cells (LOG), as shown in a Pearson correlation matrix (Fig. 1B). Thus, the massive changes in transcription do not require replication. Following nutrient feeding, a core set of roughly 500 growth genes is immediately and dramatically upregulated (Fig. 1C, top), whereas another group of nearly 500 stress genes is promptly downregulated (Fig. 1C, bottom). As expected, gene ontology (GO) enrichment analyses indicate that nutrient-induced growth genes are involved in processes critically important for growth, including ribosome biogenesis, rRNA processing, and translational regulation (Fig. 1D). In contrast, genes that are actively transcribed in quiescent cells and become rapidly downregulated after nutrient feeding are highly overrepresented in classic stress response categories, such as oxidation-reduction and response to heat (Fig. 1D).

The induction of growth genes has been shown to correlate with glucose-dependent increases in histone acetylation (10, 11). We confirmed by Western blot analysis that transcriptionally relevant histone acetylation levels drop dramatically during quiescence and then robustly and rapidly increase after nutrient refeeding as the cells exit quiescence (Fig. 1E, H4K5ac and H4K8ac; Fig. 1F, H3K9ac). Strikingly, Western blot analysis revealed that for all of the abundant methylation sites relevant to transcription (K4, K36, and K79), there was no global change during nutrient starvation and replenishment (Fig. 1E and F). Thus, in stark contrast to histone acetylation, which is connected to transcription, global histone methylation levels remain constant in nutrient-stressed quiescent cells and do not increase during nutrient-induced cell cycle reentry.

Histone methylation dynamics are distinct from those of histone acetylation during exit. While Western blot analysis measures the total relative abundance of specific histone modifications, this technique is unable to measure either turnover dynamics or changes in genome-wide distribution of those modifications. Although the kinetics in exiting cells have not been previously reported, it has been speculated that turnover dynamics of various histone modifications correspond to cellular metabolism (18, 32). To investigate methylation dynamics, we performed SILAC in quiescent and quiescence-exiting cells. To track and quantify histone protein turnover, as well as newly acetylated and methylated histones, we cultured cells in medium with isotopically heavy lysine ($[^{13}C_6, {}^{15}N_2]$lysine), glucose ($[^{13}C_6]$glucose), or methionine ($[^{13}C]D_3$-methionine), respectively, prepared nuclei, and isolated histones (Fig. 2A, left). While the stable heavy isotopes do not perturb the system (21, 33), the rate of label incorporation into histone modification pools can be monitored by tandem mass spectrometry analysis. Specific shifts in the mass-to-charge (*m/z*) ratio are used to distinguish unlabeled from labeled histone peptides and to reveal modification turnover rates when measured with respect to time of continuous isotopic labeling (Fig. 2A, right). In contrast to a shift in *m/z*, the incorporation of the heavy isotopes generally does not induce a significant shift in retention time, and thus, histone peptides with light, heavy, or a

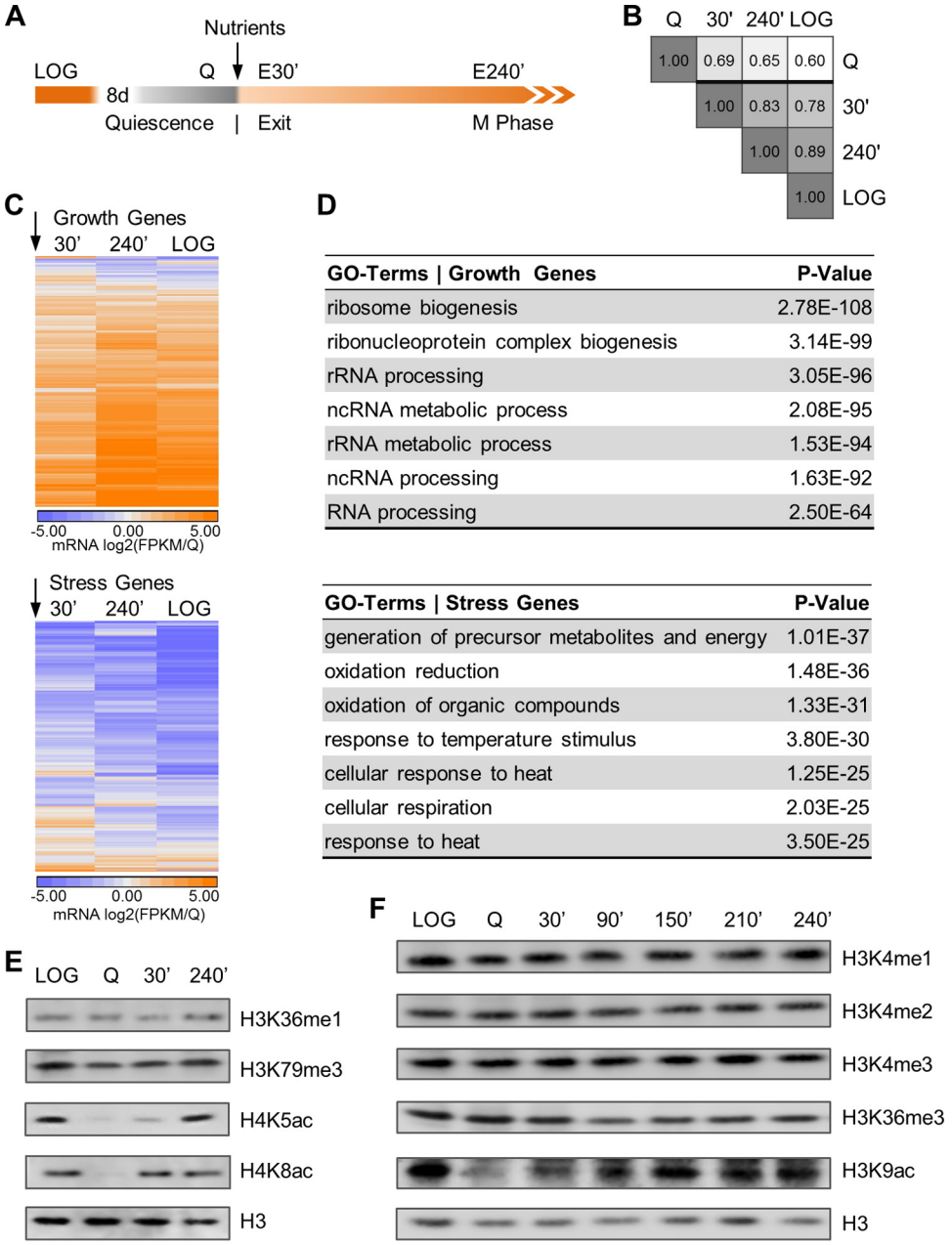

GO-Terms | Growth Genes	P-Value
ribosome biogenesis	2.78E-108
ribonucleoprotein complex biogenesis	3.14E-99
rRNA processing	3.05E-96
ncRNA metabolic process	2.08E-95
rRNA metabolic process	1.53E-94
ncRNA processing	1.63E-92
RNA processing	2.50E-64

GO-Terms | Stress Genes	P-Value
generation of precursor metabolites and energy	1.01E-37
oxidation reduction	1.48E-36
oxidation of organic compounds	1.33E-31
response to temperature stimulus	3.80E-30
cellular response to heat	1.25E-25
cellular respiration	2.03E-25
response to heat	3.50E-25

FIG 1 Nutrient availability stimulates histone acetylation and dramatic change in gene expression but does not alter global histone methylation levels. (A) Schematic of yeast culturing and quiescence exit protocol. Cells are grown in rich medium (LOG) until carbon exhaustion and are then transferred to water to ensure a completely starved, homogeneous quiescent cell population (Q) prior to nutrient-induced quiescence exit on day 8. The arrow indicates nutrient feeding and subsequent sampling 30 min and 240 min after nutrient feeding (E30′ and E240′, respectively). (B) Pearson correlation matrix of mRNA transcriptomes. In nutrient-induced cell cycle reentry, changes in global gene expression advance genome-wide transcription to the growth profile of cycling cells. (C) mRNA sequencing data show that nutrient feeding (arrows) induces vast transcriptional reprogramming in the transition from quiescence to cellular growth. Following nutrient replenishment, 475 growth genes are drastically upregulated (orange), whereas a core set of 463 stress genes are rapidly downregulated (blue). Data are clustered by time points into columns and rows; rows represent genes, which are ranked by FPKM (where FPKM stands for fragments per kilobase of transcript per million mapped reads) values normalized to quiescence sample FPKM and $\log_2$ transformed. (D) GO term enrichment analysis shows that growth genes are involved in processes critical to growth. Stress genes cluster in classic stress response categories. (E and F) Western blot analysis of lysates from yeast over the course of quiescence exit reveals that total levels of histone acetylation are diminished in quiescent cells and rapidly increase following nutrient replenishment. In contrast, global histone methylation levels remain stable throughout quiescence establishment and do not increase during quiescence exit.

combination of both isotopes generally coelute by reversed-phase liquid chromatography. By measuring the metabolic rate of labeled isotope incorporation into histone modifications, we determined the residue-specific dynamics of acetylation and methylation in the context of major transcriptional reprogramming during quiescence exit.

To establish conditions and explore histone methylation by SILAC, we first examined turnover of both histone protein and

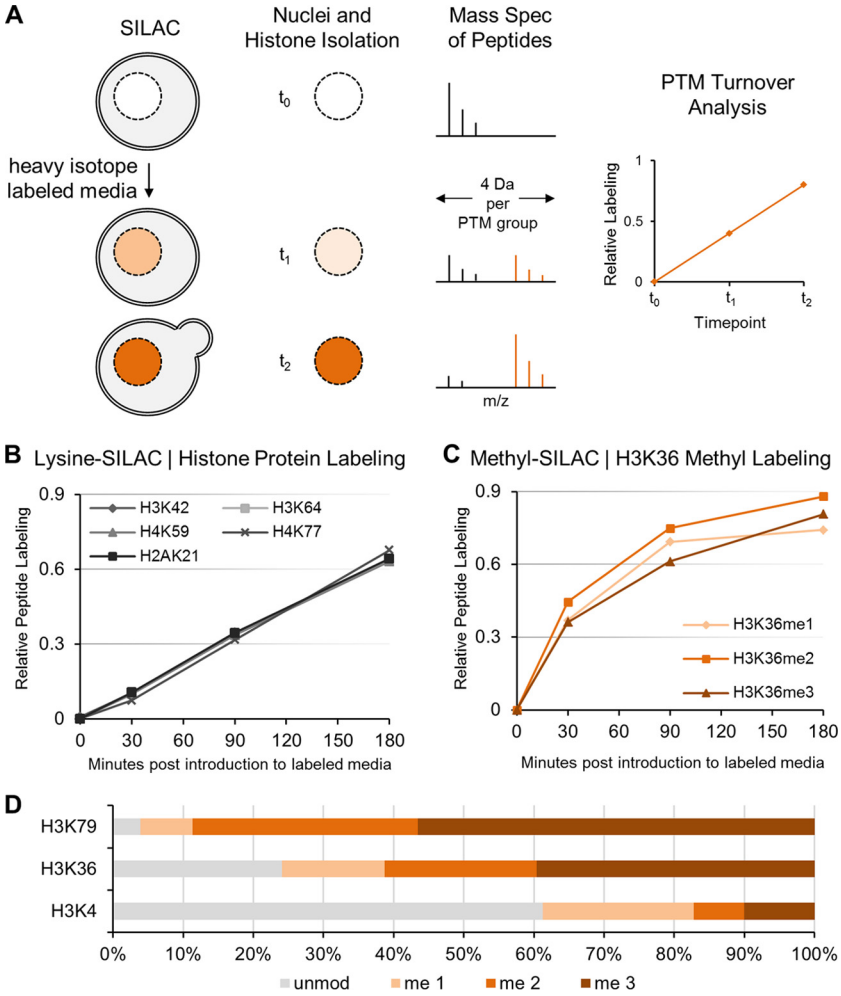

FIG 2 SILAC-mass spectrometry analysis of histone protein and methylation dynamics in proliferating cells. (A) Method of SILAC-based quantitative mass spectrometry. Cells are cultured in medium containing labeled heavy isotopes (e.g., [^{13}C]D_3-methionine to track methylation). Isotope incorporation (orange) into histone peptides or modification pools is monitored by tandem mass spectrometry analysis. Specific shifts in the mass-to-charge (*m/z*) ratio are used to distinguish unlabeled from labeled histone peptides or modifications and reveal turnover dynamics when measured over time (e.g., a 4-Da shift per methyl group). (B) SILAC with [$^{13}C_6$]-L-lysine in proliferating cells shows relative distributions and half-max labeling time of newly synthesized H3, H4, and H2A peptides, confirming doubling of the histone pool with every cell division (~130 min). (C) Methyl-SILAC with heavy [^{13}C]D_3-methionine in proliferating cells shows rapid incorporation of [^{13}C]D_3-methionine into histone methylation of H3K36 (*y* axis represents total methylation labeling; e.g., 0.9 denotes 90% labeling) (D) SILAC mass spectrometry reveals the percentage of unmodified and mono-, di-, and trimethylated histone H3 at residues K79, K36, and K4 in proliferating cells.

histone methylation in proliferating cells. First, to track turnover of histone proteins in cycling cells, we performed SILAC using heavy lysine (Fig. 2B). Following the transfer of proliferating cells to heavy medium, any histones that have incorporated isotopically heavy [$^{13}C_6$, $^{15}N_2$]lysine can be distinguished as "newly" synthesized histone proteins. We found that the half-maximal labeling time ($t_{1/2}$) of histone proteins corresponds to approximately one budding yeast cell cycle of 130 min, confirming by SILAC that doubling of the histone protein pool occurs once with every cell division (Fig. 2B).

Next, to examine residue-specific methylation dynamics in proliferating cells, we utilized heavy-methionine SILAC. This method involves mass spectrometry detection of *in vivo* incorporation of labeled *S*-adenosylmethionine (SAM), originating from metabolized exogenous [^{13}C]D_3-methionine into endogenous methylation substrates. Heavy methionine was rapidly metabolized to SAM, and we detected histone methylation labeling within minutes of transfer to heavy medium (Fig. 2C). We detected ratios of mono-, di-, and trimethylated histone H3 that are consistent with their abundance and prevalent functions at promoters (K4), over partial gene bodies (K36), and over entire gene bodies (K79) (Fig. 2D).

Having established SILAC in proliferating cells to study histone modification dynamics, we then applied this method to quiescent cells that were induced to reenter the cell cycle by nutrient feeding. First, as a control for the method, we examined glucose-dependent histone acetylation in quiescence exit by utilizing heavy glucose SILAC. By mass spectrometry, we detected a burst of histone acetylation that occurs immediately after nutrient replenishment, resulting from the glycolytic breakdown of heavy-labeled [$^{13}C_6$]glucose from fresh medium (Fig. 3A). Specifically, new histone H3K9/K14 acetylation takes place within minutes (Fig. 3A, red), thus supporting the turnover dynamics of previ-

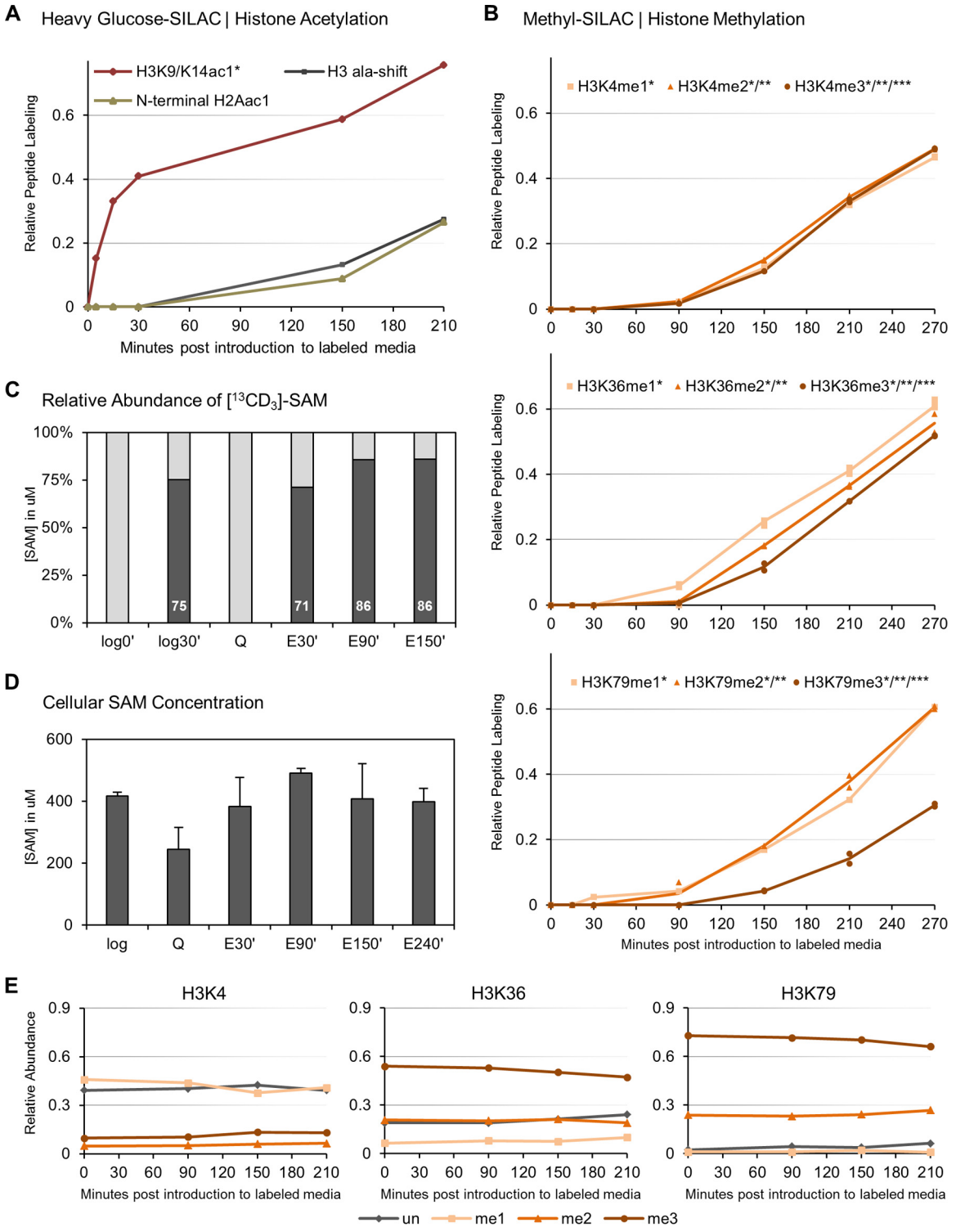

FIG 3 Histone methylation, unlike histone acetylation, remains static during quiescence exit. (A) [$^{13}C_6$]glucose-SILAC shows an immediate nutrient-induced increase in labeling of histone H3 acetylation (H3K9/K14ac1*). N-terminal histone H2A acetylation is mediated cotranslationally and becomes labeled only late in exit, concurrently with alanine labeling of newly synthesized histone proteins. (B) Methyl-SILAC during quiescence exit shows that all H3 K4, K36, and K79 methylation states remain remarkably static during nutrient-induced cell cycle reentry, and new methylation occurs only late in exit concomitantly with histone protein synthesis. (C) Mass spectrometry confirms rapid labeling of cellular SAM pools by [^{13}C]D_3-methionine in proliferating cells (log0′ and log30′) and upon nutrient replenishment in quiescent cells when histone methylation remains static. (D) Levels of methyl donor SAM were assessed. Cellular SAM levels are slightly lowered in quiescence but rise during early quiescence exit to levels characteristic of cycling cells. (E) Mass spectrometry shows that the overall levels of the corresponding methylated H3 peptides remain constant.

ously reported Western blot analyses that showed rapid increases in histone acetylation (Fig. 1E and F) (11).

We found that labeling of N-terminal histone H2A acetylation occurs only several hours into exit (Fig. 3A, blue). N-terminal acetylation is a prevalent and highly conserved eukaryotic protein modification that is mediated cotranslationally; hence, our data indicate that histone protein synthesis commences late in exit and is concurrent with DNA replication. Consistent with this observation, label incorporation into the histone protein pool via alanine residues also occurs very late upon cell cycle return (Fig. 3A, gray). These data demonstrate the absence of a slowly cycling subpopulation of cells and indicate homogeneity of the quiescent population.

We then examined histone methylation dynamics with methyl-SILAC as the cells reentered the cell cycle. Intriguingly, histone methylation remains remarkably static throughout quiescence exit. This trend was true of all H3K4, K36, and K79 methylation states, representing all of the abundant transcriptionally linked histone methylation sites in yeast (Fig. 3B). Indeed, *de novo* histone methylation occurs only late during cell cycle reentry, well after the burst of histone acetylation (compare Fig. 3B to A). We again confirmed that histone proteins are synthesized late in exit, as assessed in the above-described experiment by heavy-glucose SILAC (Fig. 3A, gray) and in the one described here by heavy-lysine SILAC (data not shown). Thus, new histone methylation occurs coincidentally with histone protein synthesis late in exit, when cells resumed replication.

We wanted to test a trivial explanation for the lack of change of methylation compared to acetylation in the early exit. It is possible that saturation of *in vivo* SAM pools with exogenous [^{13}C]D$_3$-methionine is slower than saturation of *in vivo* acetyl-CoA pools with exogenous [^{13}C$_6$]glucose in yeast cells undergoing quiescence exit. This would result in an apparently lower rate of pulse-labeling of methyl groups compared to acetyl groups. To address this, we tested by mass spectrometry of SAM whether [^{13}C]D$_3$-methionine was rapidly taken up and incorporated into SAM pools during refeeding. We found that heavy labeling of SAM occurs early in exit by 30 min (E30′ in Fig. 3C) and is comparable to labeling of SAM in cycling cells during log growth (log30′ in Fig. 3C). We further confirmed that cellular SAM levels in cells exiting quiescence are similar to proliferating cells (Fig. 3D). While the SAM concentration is slightly lower in quiescent cells, cellular SAM pools readily rise during early exit to levels typical for cycling cells (Fig. 3D), at a time when massive transcriptional changes occur in the absence of novel histone methylation, as shown by heavy-methyl SILAC (Fig. 3B). In addition to the absence of dynamic increase in histone methylation upon quiescence exit, we also noted by mass spectrometry that overall levels of the corresponding methylated peptides are constant (Fig. 3E), validating our findings by Western blot analysis (Fig. 1E and F).

The SILAC analysis shows that histone methylation is surprisingly static during quiescence exit and is wholly different from histone acetylation, which is dramatically induced during massive changes in gene expression. New histone methylation appears only late, concurrent with replication and concomitant histone protein synthesis.

Histone methylation is redistributed genome-wide during quiescence and exit. We were surprised that histone methylation remains static in the backdrop of massive metabolic and transcriptional change. While genome-wide histone acetylation patterns have been investigated in nutrient-stressed cells (11), the histone methylation status of growth and stress genes during quiescence and exit is unknown. We investigated the genome-wide distribution of histone modifications during quiescence and exit, focusing on two core groups of genes that have been previously described by microarray analysis as prominently transcribed during growth and during nutrient stress (5, 6, 34), which we confirmed by our RNA analysis (Fig. 1C and D).

We performed ChIP-seq in the same time course to examine and compare histone acetylation and histone methylation. Histone acetylation at growth genes becomes greatly diminished in quiescence (Fig. 4A, left). When these growth genes are induced upon nutrient replenishment, H3K9ac (Fig. 4A, left) and H4K12ac (Fig. 4B, left) rapidly increase at these loci. In contrast, H3K9ac and H4K12ac in quiescent cells are enriched at stress genes that are induced upon nutrient starvation and then diminish in E30, E240, and LOG samples (Fig. 4A and B, right). Thus, our findings confirm observations previously made under similar conditions of nutrient limitation and environmental stress (10).

We then analyzed genome-wide enrichment patterns of H3K4me3 and H3K36me3, which are associated with active gene expression. While overall global methylation levels remained stable, as shown by Western blot analysis and mass spectrometry (Fig. 1F and 3E), we detected genome-wide shifts in the methylation status of growth and stress genes when we compared cells that had gone through the long process of establishing the quiescent state: note that the dotted and red lines (LOG and E240) are distinct from the blue and orange lines (Q and E30) (Fig. 4C and D). Specifically, histone methylation at growth genes is decreased during quiescence (Fig. 4C and D, left), whereas methylation at stress genes is increased (Fig. 4C and D, right). Strikingly, this new methylation pattern established during quiescence remains largely intact through early exit (i.e., the Q and E30 lines are very similar) despite the enormous changes in transcription and histone acetylation that occur after refeeding (Fig. 1). We do note that, at stress genes, H3K4me3 drops partially at E30, which might be related to the downregulation of these genes as the cells leave quiescence. Importantly, new histone methylation at growth genes occurs only during late exit (E240), when the cell cycle is fully engaged (Fig. 4C and D, left). To confirm these genome-wide methylation data, we performed ChIP qRT-PCR in a time course for H3K4me3 and H3K36me3 for individual growth and stress genes (data not shown).

The clear quantitative contrast between genome-wide acetylation and methylation is most easily visualized by box plot analysis (Fig. 5). H3K9ac drops at stress genes between Q and E30 and increases at growth genes between Q and E30. In contrast, H3K4me3 and K36me3 remain constant at both stress and growth genes between Q and E30. Importantly, these ChIP-seq findings for histone methylation agree with our methyl-SILAC data showing that catalytic histone methylation is altered late (at E240) but not early (at E30) after quiescence exit (Fig. 3B).

Indeed, further analysis of the ChIP-seq histone modification profiles at growth genes confirms stark dissimilarities during exit. The dynamic histone acetylation profiles at these genes correlate with gene expression changes upon nutrient-induced cell cycle reentry (Fig. 1C and 6A). In proliferating cells, such a correlation is also found between histone methylation and growth gene expression (Fig. 1C and 6B, left). However, the altered methylation profiles in the quiescent state (Q) remain unchanged in the early-

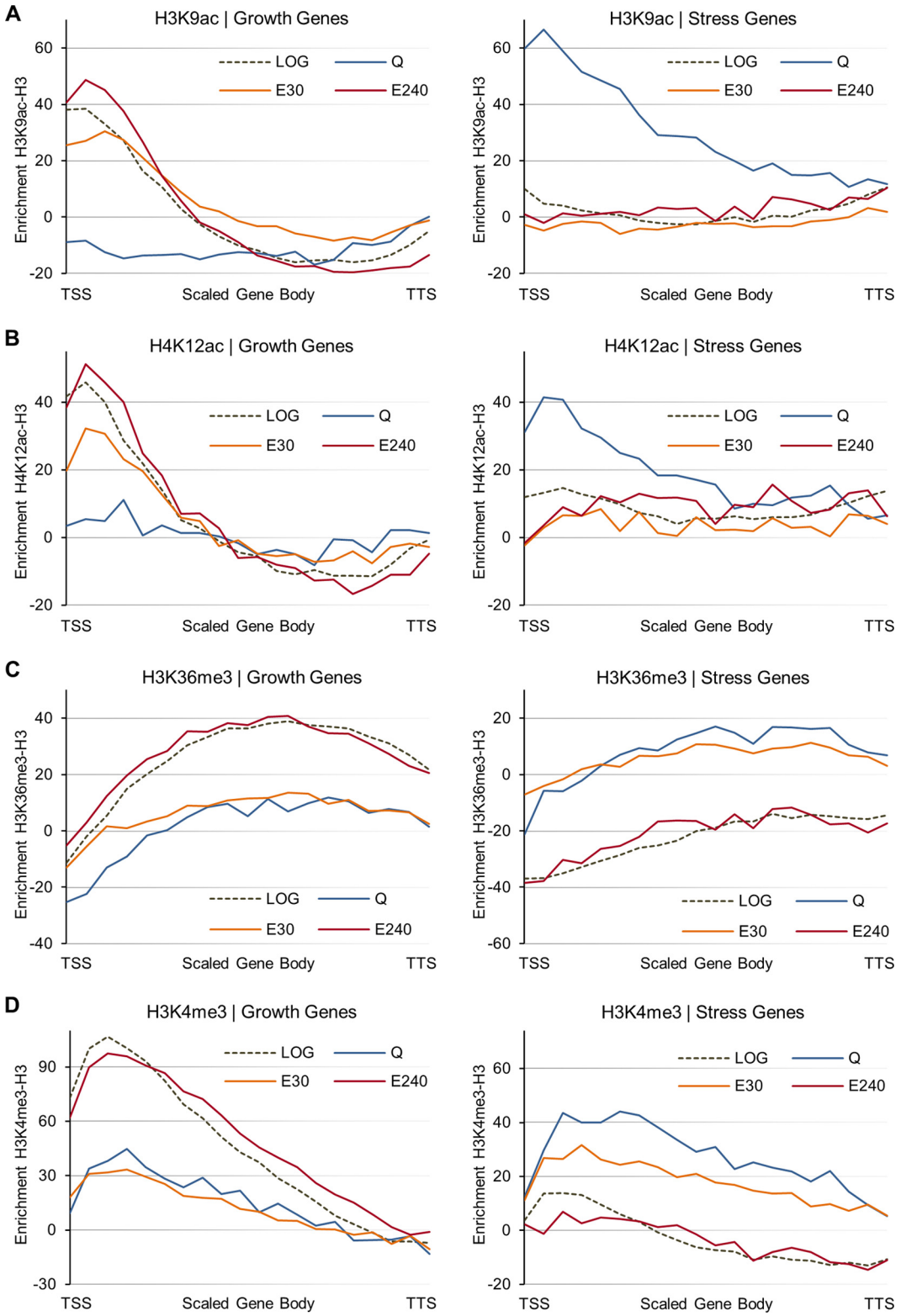

FIG 4 Histone methylation is redistributed as proliferating cells enter quiescence but remains static in early exit from quiescence. Average ChIP-seq enrichment of H3K9ac (A), H4K12ac (B), H3K36me3 (C), and H3K4me3 (D) over scaled bodies (from the transcriptional start site [TSS] to the transcriptional termination site [TTS]) of all growth and stress genes characterized in Fig. 1 reveals differences between histone acetylation and methylation levels at these two distinct gene groups during quiescence establishment and exit. The histone modification ChIP signal was normalized to the H3 ChIP signal.

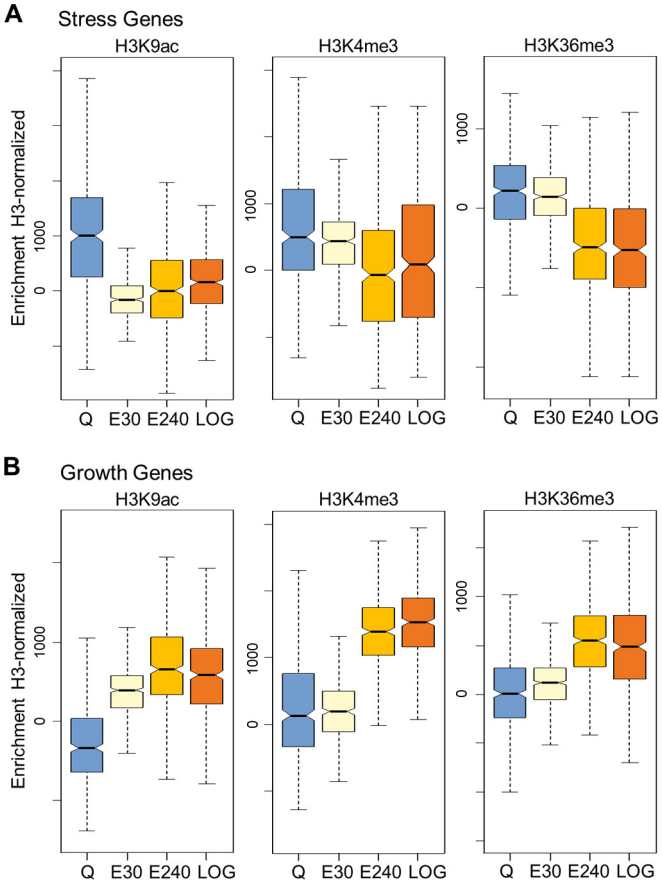

FIG 5 Box plot analysis shows distinct dynamics of histone acetylation and methylation at growth and stress genes during the early exit. H3K9ac drops at stress genes (A) between Q and E30 and increases at growth genes (B) between Q and E30. In contrast, H3K4me3 and K36me3 remain constant at both stress and growth genes between Q and E30.

exit (E30) samples: even though both acetylation and expression of growth genes are greatly increased in the early-exit samples, their methylation profiles remain unchanged (Fig. 6B, right) and do not correlate with gene expression in the early-exit samples (Fig. 6C).

We then investigated histone acetylation and methylation in another group of environmentally regulated genes that was previously found to exhibit highly dynamic and stress-responsive histone acetylation induced by H_2O_2 treatment (35, 36). Again, we found that histone acetylation is rapidly increased at E30 upon nutrient replenishment, whereas histone methylation remains static and does not follow these dynamics (data not shown). As a control, we determined that neither histone acetylation or methylation changes at nutrient-insensitive genes during early exit (E30) (data not shown).

We then examined methylation patterns over 1-kilobase windows genome-wide in Q, E30, E240, and LOG samples by scatterplot analysis. As expected from the box plot analysis, methylation patterns are highly correlated between E240 and LOG and between Q and E30 but are very different between Q and LOG (Fig. 7A, top). Prominently, the correlation of genome-wide H3K36 methylation between Q and E30 (Fig. 7A, top right) is strikingly contrasted by the highly dissimilar H3K9 acetylation patterns between Q and E30 cells (Fig. 7A, lower right).

We further investigated the relationship of histone methylation enrichment to different gene families, examining H3K36me3 during LOG, Q, E30, and E240 using unbiased gene ontology (GO) enrichment analysis. We queried GO terms that link to the top methylated genes; we found that LOG cells and E240 cells share categories that are related to cell growth and proliferation (Fig. 7B, left, red and gray circles). Remarkably, genes that are methylated in Q and E30 share GO terms associated with stress (Fig. 7B, left, blue and orange circles), despite their decidedly distinct expression and histone acetylation profiles. In contrast, GO terms that link to the top acetylated genes in Q do not overlap GO terms associated with genes that are acetylated in early exit (E30) (Fig. 7B, right).

Thus, by ChIP-seq, we uncovered genome-wide changes in histone methylation that are obscured in Western and SILAC analyses. First, our genome-wide analysis revealed that during quiescence establishment, stress genes become methylated when their expression is induced, whereas growth genes experience extensive methylation losses when they are not transcribed. Second, during exit, ChIP-seq revealed two key features of the location of dynamic histone methylation changes determined by SILAC: (i) quiescence-specific methylation patterns remain remarkably intact through early exit (E30), but (ii) they change in the course of

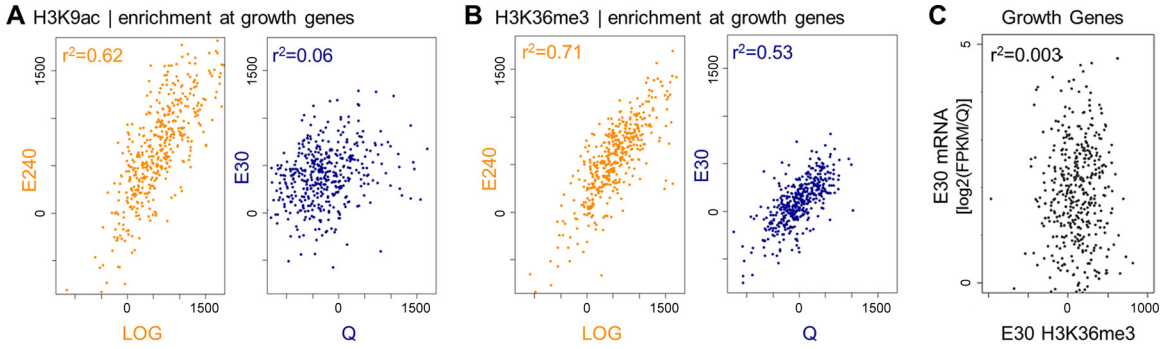

FIG 6 Scatterplot analyses demonstrate distinct dynamics of histone acetylation and methylation at growth genes. (A and B) Scatterplots contrasting the enrichment of H3K9ac (A) and H3K36me3 (B) at growth genes: histone acetylation correlates well between LOG and E240 cells (A, orange) but not between Q and E30 cells (A, blue). In contrast, histone methylation correlates well not only between the LOG and E240 time points (B, orange) but also between Q and E30 (B, blue), which shows that histone methylation remains static in early exit. (C) Growth gene expression levels (*y* axis) and H3K36me3 enrichment (*x* axis) do not correlate in the early exit from quiescence when growth genes are induced and methylation remains stable. Each dot represents one growth gene.

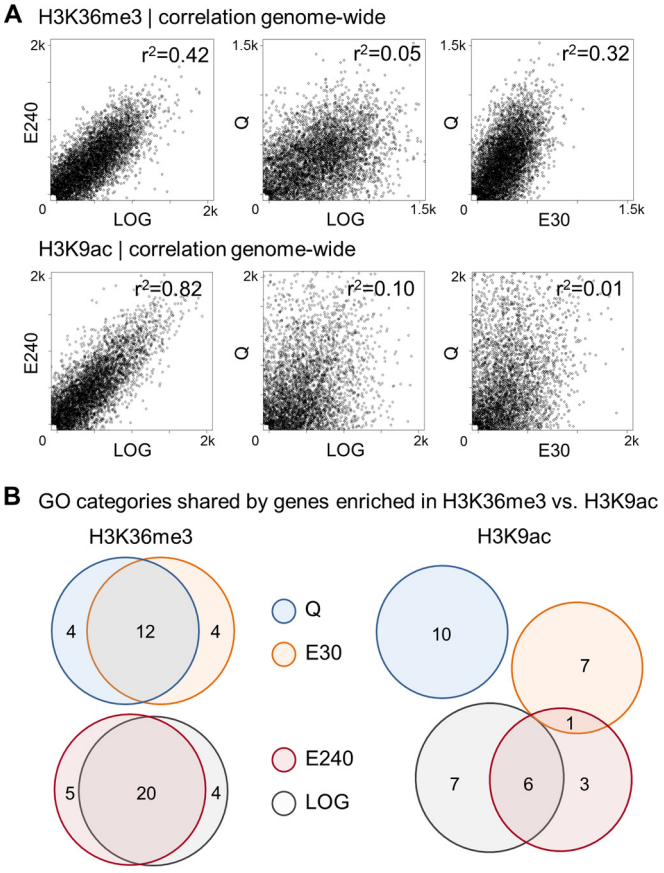

FIG 7 Histone methylation patterns show correlation genome-wide during quiescence exit. (A) Genome-wide ChIP-seq enrichment correlations can be seen between proliferating cells (LOG) and cells in late quiescence exit (E240) for both H3K36me3 and H3K9ac. The H3K36me3, but not H3K9ac, enrichment pattern is highly correlated in quiescence (Q) and early exit (E30). Each dot represents a 1,000-bp window of the genome. (B) Genes enriched for H3K36me3 in proliferating cells (LOG) and genes methylated in late exit cells (E240) cluster into shared GO categories (data not shown; categories are related to growth, e.g., regulation of translation, ribosome biogenesis, and nuclear export). Genes that are methylated in quiescent (Q) and early-exit (E30) cells also share GO categories (related to stress, e.g., cell death and response to abiotic stimuli). Genes enriched for H3K9ac in quiescent cells (Q) cluster into stress categories that are not shared by genes that are acetylated in E30, E240, or LOG (data not shown). Genes that are acetylated in E240 and LOG cluster into shared categories that are linked to ribosome biogenesis and translational regulation.

replication initiation at E240, when *de novo* histone methylation occurs exclusively at growth genes. These results, taken together with our SILAC analyses described above, underscore the differences in the roles of histone methylation and acetylation in the dramatic gene expression changes following quiescence exit. Histone acetylation rapidly responds to metabolic state, but histone methylation remains stable through quiescence exit and undergoes genome-wide redistribution, with *de novo* growth gene methylation being linked to the initiation of cellular replication.

DISCUSSION

The epigenome is hypothesized to provide an interface between the cellular environment and gene expression. One of the most important environmental factors that must be synchronized with gene transcription is the availability of caloric energy. Indeed, glucose-derived acetyl-CoA is thought to function as a modulator of histone acetylation and growth-related gene expression (10). Previous studies suggest that histone acetylation is exquisitely responsive to the nutritional state of cells. In fact, our findings from SILAC demonstrate that certain histone acetylation sites and, by default, their acetylation enzymes operate as bona fide energy sensors, providing unequivocal evidence that nutrients induce an immediate histone acetylation response, driven by external glucose (Fig. 3A).

Histone methylation also has an important role in gene regulation in all eukaryotes. Chemically, methylation is more stable than acetylation and is known to be less dynamic in cells. Hence, a key question is whether histone methylation responds to nutritional status. Like histone acetylation, histone methylation is speculated to be synchronized with metabolic information in order to regulate gene expression (8, 18, 37). Here, we performed a comprehensive investigation of methylation profiles during quiescence exit, when cells undergo a dramatic shift in gene regulation as a result of the drastic change in metabolic state from nutrient starvation into regrowth. We observe that histones become enriched for acetylation at certain genes both globally (by Western blot) and locally (by ChIP-seq). Indeed, similar observations have constituted a paradigm for how metabolic changes can alter the epigenome (10, 11). Our rigorous examination, additionally by SILAC, fully confirms that histone acetylation responds immediately to increased nutrition after starvation. Thus, this nutrient-induced transition from quiescence to proliferation represents an ideal scenario to examine signaling from the metabolic state to histone methylation.

Histone methylation as an epigenetic memory mark during metabolic shifts in cell cycle reentry. To investigate histone methylation during quiescence exit, we used three approaches: (i) Western blot analysis with methyl-specific antibodies, as was previously used to demonstrate global changes in histone acetylation (11); (ii) quantitative mass spectroscopy using heavy-labeled precursors to distinguish new histone methylation immediately following refeeding; and (iii) ChIP-seq with methyl-specific antibodies, as was previously used to examine site-specific acetylation in metabolic cycling yeast (10). Interestingly, we found that histone methylation, irrespective of the residue or methylation states, is exceptionally stable and is uncoupled from rapid changes in the metabolic state as cells exit quiescence (Fig. 3B). Western blotting and SILAC showed that the overall global levels of methylation do not change and do not turn over as the cells emerge from quiescence. Furthermore, ChIP-seq revealed that there are no localized changes in genomic distribution during quiescence exit until cell replication commences. In contrast, these same approaches provide clear evidence that histone acetylation is dynamic: new acetylation is detected by SILAC immediately following refeeding and well before replication (Fig. 4). Finally, ChIP-seq shows that acetylation is rapidly enriched at genes that are induced and depleted at genes that are repressed.

Thus, our observations revealed that yeast cells that return to the cell cycle under nutrient-rich conditions exhibit a strikingly stable methylation landscape despite major metabolic and transcriptional reprogramming. Historically, histone methylation has been thought to be a static modification, based on studies that have demonstrated similar turnover rates for methyl groups and histone proteins (38, 39); however, in the past decade, the notion that histone methylation is enzymatically irreversible has been

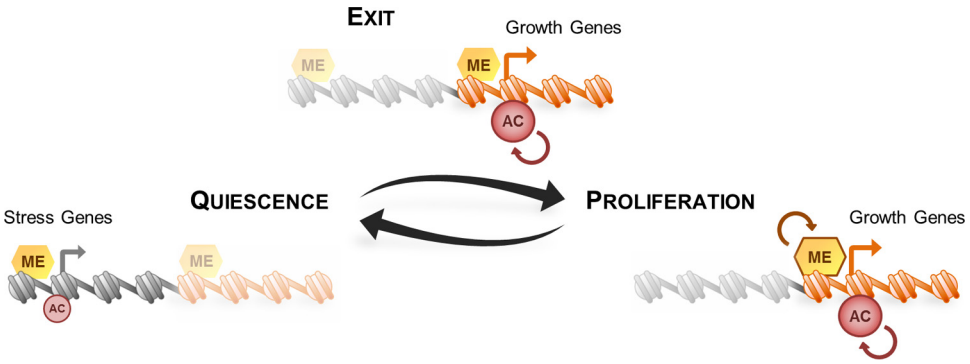

FIG 8 Schematic model for the distinct dynamics of histone methylation and acetylation during quiescence establishment and exit. The methylation landscape is changed genome-wide in cellular quiescence. In nutrient-induced cell cycle reentry, this methylation pattern remains strikingly intact, in contrast to dynamic histone acetylation, which is linked to gene transcription. Upon cell cycle return, the methylation landscape is restructured only very late in conjunction with genome replication and ensuing cell division.

challenged by the identification of numerous HDMs, specifically, the lysine-specific demethylase 1 (LSD1) and Jumonji C demethylases (40–42). Remarkably, both domain classes of HDMs require high-energy metabolic cofactors—flavin adenine dinucleotide (FAD) and α-ketoglutarate, respectively. Thus, the coenzymes of both HMTs and HDMs are positively regulated by high energy levels, an apparent paradox that likely imposes further regulation should these enzymes be integrated in metabolic control. In contrast, HATs and HDACs are regulated by high and low energy levels, respectively, adapting histone acetylation to dynamic metabolic processes through acetyl-CoA generation and the cellular redox state.

Our results confirm that histone acetylation quickly drives growth gene transcription in relation to transient caloric availability when emerging from quiescence, whereas histone methylation remains surprisingly static during the early exit (Fig. 8). We cannot exclude the possibility that metabolic fluxes directly modify methylation later, i.e., during cell replication when we detect new methylation. Thus, histone methylation may not play a role in the initial reactivation of growth genes but may function in the late cell cycle reentry to provide transcriptional marking and coordinate gene expression following genome replication. This is a particularly intriguing possibility, given our observation of *de novo* methylation late after quiescence exit.

Furthermore, our results show that histone methylation is indicative of transcriptional potential but not necessarily current transcriptional activity. Indeed, we confirm that enrichment of H3K4me3 at promoters correlates with gene activity in proliferating yeast (43, 44); however, we also show that H3K4me3 does not directly correlate with gene expression in the quiescent cell state, (i.e., we detect H3K4me3 at both active stress genes and inactive growth genes). In fact, previous observations in mammalian cells showed that H3K4me3 is actually present at a majority of promoters and is not strictly predictive of transcriptional activity (45, 46).

In summary, we find that acetylation is lost nearly completely at growth genes during quiescence and—driven by metabolic state—is very rapidly reinstated in early exit. In contrast, full remethylation at growth genes occurs only at the time of cell replication following quiescence exit. Accordingly, although diet, exercise, and circadian rhythms are all known to readily manipulate histone acetylation to maintain metabolic homeostasis, they may not easily modify long-term histone methylation.

Histone methylation in the context of altered metabolism in cancer and stem cell populations. It is interesting to compare our results with recent investigations of histone methylation in higher eukaryotic cells in the context of proliferative states. In many cancers, deregulated histone methylation has been implicated in tumorigenesis (47, 48). In a variety of tumors, the metabolic enzymes isocitrate dehydrogenase 1 (IDH1) and IDH2 were found to bear mutations that result in neomorphic activities that generate 2-hydroxyglutarate (2HG) (49). As an oncometabolite, 2HG inhibits a family of Jumonji C domain histone demethylases (JHDMs) and is thought to disrupt gene expression patterns through alterations in the histone methylation landscape (49).

In addition, recent findings suggest a mechanistic link between reprogrammed cancer metabolism and an altered methylation landscape (50). Certain cancer cells aberrantly express high levels of the metabolic enzyme nicotinamide *N*-methyltransferase (NNMT) and exhibit global methylation defects when methionine is limited. Under these conditions, the increased catalytic capacity of NNMT may drain cellular SAM pools by creating stable 1-methylnicotinamide and thereby impair histone and other protein methylation (50). However, it is unclear when, during the cell cycle, elevated NNMT activities may actually affect histone methylation and how broad alterations in the methylation landscape eventually promote oncogenesis. Therefore, in order to develop novel therapeutic approaches that target cellular metabolism and alter the tumor epigenome, it is key to understand how chromatin may be metabolically regulated in noncancerous cells.

Interestingly, histone methylation not only may be influenced by metabolic alterations in tumors but also may be manipulated by metabolic adaptations in stem cells, where methylation has critical functions in transcriptional regulation and self-renewal (51, 52). Current evidence suggests that the pluripotency of mouse embryonic stem cells (mESCs) is dependent on their distinct mode of threonine catabolism and its effect on SAM metabolism and H3K4me3 (20). When proliferating mESCs are cultured in threonine-depleted medium, SAM levels become lowered and H3K4me3 levels—but not levels of other methylation—decrease, which results in slowed growth and increased differentiation (20). However, as threonine dependency is specific to mouse ESCs, it remains unclear whether histone methylation is similarly influenced by metabolic activities in other stem cell populations, like human ESCs or adult human stem cells. Notably, histone methyl-

ation may be under metabolic influence only at specific times, e.g., when quiescent adult human stem cells are induced to return to the cell cycle and initiate cell replication for clonal expansion.

From our findings in the yeast model, histone methylation may also have functions distinct from those of histone acetylation in the orchestrated cell cycle reentry in induced stem cells, fibroblasts, or lymphocytes. Unlike acetylation, methylation may regulate gene expression independently of the metabolic milieu during early cell cycle return. Rather, it may function as an epigenetic marker of cellular transcriptional identity during genome replication and cell division.

ACKNOWLEDGMENTS

We thank J. Rabinowitz and his laboratory for their generous help and Wenyun Lu in particular for the SRM analysis. We thank Leila Afjehi-Sadat for sharing both her insight and the benzoic anhydride peptide preparation protocol. We thank the IDOM Functional Genomics Core Sequencing Facility for RNA-seq and ChIP-seq.

This work was supported by an NIA P01 grant (P01AG031862) and Ellison Foundation Senior Scholar award to S.L.B.

REFERENCES

1. **Sang L, Coller HA, Roberts JM.** 2008. Control of the reversibility of cellular quiescence by the transcriptional repressor HES1. Science **321:**1095–1100. http://dx.doi.org/10.1126/science.1155998.
2. **Pardee AB.** 1974. A restriction point for control of normal animal cell proliferation. Proc. Natl. Acad. Sci. U. S. A. **71:**1286–1290. http://dx.doi.org/10.1073/pnas.71.4.1286.
3. **Gray JV, Petsko GA, Johnston GC, Ringe D, Singer RA, Werner-Washburne M.** 2004. "Sleeping Beauty": Quiescence in Saccharomyces cerevisiae. Microbiol. Mol. Biol. Rev. **68:**187–206. http://dx.doi.org/10.1128/MMBR.68.2.187-206.2004.
4. **Martinez MJ, Roy S, Archuletta AB, Wentzell PD, Anna-arriola SS, Rodriguez AL, Aragon AD, Quin GA, Allen C, Werner-washburne M.** 2004. Genomic analysis of stationary-phase and exit in Saccharomyces cerevisiae: gene expression and identification of novel essential genes. Mol. Biol. Cell **15:**5295–5305. http://dx.doi.org/10.1091/mbc.E03-11-0856.
5. **Slattery MG, Heideman W.** 2007. Coordinated regulation of growth genes in Saccharomyces cerevisiae. Cell Cycle 1210–1219. http://dx.doi.org/10.4161/cc.6.10.4257.
6. **Radonjic M, Andrau J-C, Lijnzaad P, Kemmeren P, Kockelkorn TTJP, van Leenen D, van Berkum NL, Holstege FCP.** 2005. Genome-wide analyses reveal RNA polymerase II located upstream of genes poised for rapid response upon S. cerevisiae stationary phase exit. Mol. Cell **18:**171–183. http://dx.doi.org/10.1016/j.molcel.2005.03.010.
7. **Kaelin WG, McKnight SL.** 2013. Influence of metabolism on epigenetics and disease. Cell **153:**56–69. http://dx.doi.org/10.1016/j.cell.2013.03.004.
8. **Lu C, Thompson CB.** 2012. Metabolic regulation of epigenetics. Cell Metab. **16:**9–17. http://dx.doi.org/10.1016/j.cmet.2012.06.001.
9. **Laporte D, Lebaudy A, Sahin A, Pinson B, Ceschin J, Daignan-Fornier B, Sagot I.** 2011. Metabolic status rather than cell cycle signals control quiescence entry and exit. J. Cell Biol. **192:**949–957. http://dx.doi.org/10.1083/jcb.201009028.
10. **Cai L, Sutter BM, Li B, Tu BP.** 2011. Acetyl-CoA induces cell growth and proliferation by promoting the acetylation of histones at growth genes. Mol. Cell **42:**426–437. http://dx.doi.org/10.1016/j.molcel.2011.05.004.
11. **Friis RMN, Wu BP, Reinke SN, Hockman DJ, Sykes BD, Schultz MC.** 2009. A glycolytic burst drives glucose induction of global histone acetylation by picNuA4 and SAGA. Nucleic Acids Res. **37:**3969–3980. http://dx.doi.org/10.1093/nar/gkp270.
12. **Fox CJ, Hammerman PS, Thompson CB.** 2005. Fuel feeds function: energy metabolism and the T-cell response. Nat. Rev. Immunol. **5:**844–852. http://dx.doi.org/10.1038/nri1710.
13. **Taplick J, Kurtev V, Lagger G, Seiser C.** 1998. Histone H4 acetylation during interleukin-2 stimulation of mouse T cells. FEBS Lett. **436:**349–352. http://dx.doi.org/10.1016/S0014-5793(98)01164-8.
14. **Wellen KE, Hatzivassiliou G, Sachdeva UM, Bui TV, Cross JR, Thompson CB.** 2009. ATP-citrate lyase links cellular metabolism to histone acetylation. Science **324:**1076–1080. http://dx.doi.org/10.1126/science.1164097.
15. **Katada S, Imhof A, Sassone-Corsi P.** 2012. Connecting threads: epigenetics and metabolism. Cell **148:**24–28. http://dx.doi.org/10.1016/j.cell.2012.01.001.
16. **Everts AG, Zee BM, Dimaggio PA, Gonzales-Cope M, Coller HA, Garcia BA.** 2013. Quantitative dynamics of the link between cellular metabolism and histone acetylation. J. Biol. Chem. **288:**12142–12151. http://dx.doi.org/10.1074/jbc.M112.428318.
17. **Klose RJ, Zhang Y.** 2007. Regulation of histone methylation by demethylimination and demethylation. Nat. Rev. Mol. Cell Biol. **8:**307–318. http://dx.doi.org/10.1038/nrm2143.
18. **Teperino R, Schoonjans K, Auwerx J.** 2010. Histone methyl transferases and demethylases; can they link metabolism and transcription? Cell Metab. **12:**321–327. http://dx.doi.org/10.1016/j.cmet.2010.09.004.
19. **Katoh Y, Ikura T, Hoshikawa Y, Tashiro S, Ito T, Ohta M, Kera Y, Noda T, Igarashi K.** 2011. Methionine adenosyltransferase II serves as a transcriptional corepressor of Maf oncoprotein. Mol. Cell **41:**554–566. http://dx.doi.org/10.1016/j.molcel.2011.02.018.
20. **Shyh-Chang N, Locasale JW, Lyssiotis CA, Zheng Y, Teo RY, Ratanasirintrawoot S, Zhang J, Onder T, Unternaehrer JJ, Zhu H, Asara JM, Daley GQ, Cantley LC.** 2013. Influence of threonine metabolism on S-adenosylmethionine and histone methylation. Science **339:**222–226. http://dx.doi.org/10.1126/science.1226603.
21. **Zee BM, Levin RS, Xu B, LeRoy G, Wingreen NS, Garcia Ba.** 2010. In vivo residue-specific histone methylation dynamics. J. Biol. Chem. **285:**3341–3350. http://dx.doi.org/10.1074/jbc.M109.063784.
22. **Fabrizio P, Longo VD.** 2003. The chronological life span of Saccharomyces cerevisiae. Aging Cell **2:**73–81. http://dx.doi.org/10.1046/j.1474-9728.2003.00033.x.
23. **Kizer KO, Xiao T, Strahl BD.** 2006. Accelerated nuclei preparation and methods for analysis of histone modifications in yeast. Methods **40:**296–302. http://dx.doi.org/10.1016/j.ymeth.2006.06.022.
24. **Recht J, Tsubota T, Tanny JC, Diaz RL, Berger JM, Zhang X, Garcia BA, Shabanowitz J, Burlingame A, Hunt LDF, Kaufman PD, Allis CD.** 2006. Histone chaperone Asf1 is required for histone H3 lysine 56 acetylation, a modification associated with S phase in mitosis and meiosis. Proc. Natl. Acad. Sci. U. S. A. **103:**6988–6993. http://dx.doi.org/10.1073/pnas.0601676103.
25. **Lin S, Garcia Ba.** 2012. Examining histone posttranslational modification patterns by high-resolution mass spectrometry. Methods Enzymol. **512:**3–28. http://dx.doi.org/10.1016/B978-0-12-391940-3.00001-9.
26. **Bajad SU, Lu W, Kimball EH, Yuan J, Peterson C, Rabinowitz JD.** 2006. Separation and quantitation of water soluble cellular metabolites by hydrophilic interaction chromatography-tandem mass spectrometry. J. Chromatogr. A **1125:**76–88. http://dx.doi.org/10.1016/j.chroma.2006.05.019.
27. **Zee BM, Britton L-MP, Wolle D, Haberman DM, Garcia BA.** 2012. Origins and formation of histone methylation across the human cell cycle. Mol. Cell. Biol. **32:**2503–2514. http://dx.doi.org/10.1128/MCB.06673-11.
28. **Trapnell C, Pachter L, Salzberg SL.** 2009. TopHat: discovering splice junctions with RNA-Seq. Bioinformatics **25:**1105–1111. http://dx.doi.org/10.1093/bioinformatics/btp120.
29. **Trapnell C, Williams BA, Pertea G, Mortazavi A, Kwan G, van Baren MJ, Salzberg SL, Wold BJ, Pachter L.** 2010. Transcript assembly and quantification by RNA-Seq reveals unannotated transcripts and isoform switching during cell differentiation. Nat. Biotechnol. **28:**511–515. http://dx.doi.org/10.1038/nbt.1621.
30. **Wyce A, Xiao T, Whelan KA, Kosman C, Walter W, Eick D, Hughes TR, Krogan NJ, Strahl BD, Berger SL.** 2007. H2B ubiquitylation acts as a barrier to Ctk1 nucleosomal recruitment prior to removal by Ubp8 within a SAGA-related complex. Mol. Cell **27:**275–288. http://dx.doi.org/10.1016/j.molcel.2007.01.035.
31. **Langmead B, Trapnell C, Pop M, Salzberg SL.** 2009. Ultrafast and memory-efficient alignment of short DNA sequences to the human genome. Genome Biol. **10:**R25. http://dx.doi.org/10.1186/gb-2009-10-3-r25.
32. **Katada S, Imhof A, Sassone-Corsi P.** 2012. Connecting threads: epigenetics and metabolism. Cell **148:**24–28. http://dx.doi.org/10.1016/j.cell.2012.01.001.
33. **Ong S-E.** 2002. Stable isotope labeling by amino acids in cell culture, SILAC, as a simple and accurate approach to expression proteomics. Mol.

Cell Proteomics **1:**376–386. http://dx.doi.org/10.1074/mcp.M200025-MCP200.
34. **Wang Y, Pierce M, Schneper L, Güldal CG, Zhang X, Tavazoie S, Broach JR.** 2004. Ras and Gpa2 mediate one branch of a redundant glucose signaling pathway in yeast. PLoS Biol. **2:**E128. http://dx.doi.org/10.1371/journal.pbio.0020128.
35. **Gasch AP, Spellman PT, Kao CM, Carmel-Harel O, Eisen MB, Storz G, Botstein D, Brown PO.** 2000. Genomic expression programs in the response of yeast cells to environmental changes. Mol. Biol. Cell **11:**4241–4257. http://dx.doi.org/10.1091/mbc.11.12.4241.
36. **Slattery M, Heideman W.** 2007. Coordinated regulation of growth genes in Saccharomyces cerevisiae. Cell Cycle **6:**1210–1219. http://dx.doi.org/10.4161/cc.6.10.4257.
37. **Gut P, Verdin E.** 2013. The nexus of chromatin regulation and intermediary metabolism. Nature **502:**489–498. http://dx.doi.org/10.1038/nature12752.
38. **Byvoet P, Shepherd GR, Hardin JM, Noland BJ.** 1972. The distribution and turnover of labeled methyl groups in histone fractions of cultured mammalian cells. Arch. Biochem. Biophys. **148:**558–567. http://dx.doi.org/10.1016/0003-9861(72)90174-9.
39. **Byvoet P.** 1972. In vivo turnover and distribution of radio-N-methyl in arginine-rich histones from rat tissues. Arch. Biochem. Biophys. **152:**887–888. http://dx.doi.org/10.1016/0003-9861(72)90286-X.
40. **Anand R, Marmorstein R.** 2007. Structure and mechanism of lysine-specific demethylase enzymes. J. Biol. Chem. **282:**35425–35429. http://dx.doi.org/10.1074/jbc.R700027200.
41. **Tsukada Y, Fang J, Erdjument-Bromage H, Warren ME, Borchers CH, Tempst P, Zhang Y.** 2006. Histone demethylation by a family of JmjC domain-containing proteins. Nature **439:**811–816. http://dx.doi.org/10.1038/nature04433.
42. **Smith BC, Denu JM.** 2009. Chemical mechanisms of histone lysine and arginine modifications. Biochim. Biophys. Acta **1789:**45–57. http://dx.doi.org/10.1016/j.bbagrm.2008.06.005.
43. **Pokholok DK, Harbison CT, Levine S, Cole M, Hannett NM, Lee TI, Bell GW, Walker K, Rolfe PA, Herbolsheimer E, Zeitlinger J, Lewitter F, Gifford DK, Young Ra.** 2005. Genome-wide map of nucleosome acetylation and methylation in yeast. Cell **122:**517–527. http://dx.doi.org/10.1016/j.cell.2005.06.026.
44. **Li B, Carey M, Workman JL.** 2007. The role of chromatin during transcription. Cell **128:**707–719. http://dx.doi.org/10.1016/j.cell.2007.01.015.
45. **Heintzman ND, Stuart RK, Hon G, Fu Y, Ching CW, Hawkins RD, Barrera LO, Van Calcar S, Qu C, Ching KA, Wang W, Weng Z, Green RD, Crawford GE, Ren B.** 2007. Distinct and predictive chromatin signatures of transcriptional promoters and enhancers in the human genome. Nat. Genet. **39:**311–318. http://dx.doi.org/10.1038/ng1966.
46. **Guenther MG, Levine SS, Boyer LA, Jaenisch R, Young Ra.** 2007. A chromatin landmark and transcription initiation at most promoters in human cells. Cell **130:**77–88. http://dx.doi.org/10.1016/j.cell.2007.05.042.
47. **Chi P, Allis CD, Wang GG.** 2010. Covalent histone modifications–miswritten, misinterpreted and mis-erased in human cancers. Nat. Rev. Cancer **10:**457–469. http://dx.doi.org/10.1038/nrc2876.
48. **Greer EL, Shi Y.** 2012. Histone methylation: a dynamic mark in health, disease and inheritance. Nat. Rev. Genet. **13:**343–357. http://dx.doi.org/10.1038/nrg3173.
49. **Lu C, Ward PS, Kapoor GS, Rohle D, Turcan S, Abdel-Wahab O, Edwards CR, Khanin R, Figueroa ME, Melnick A, Wellen KE, O'Rourke DM, Berger SL, Chan TA, Levine RL, Mellinghoff IK, Thompson CB.** 2012. IDH mutation impairs histone demethylation and results in a block to cell differentiation. Nature **483:**474–478. http://dx.doi.org/10.1038/nature10860.
50. **Ulanovskaya OA, Zuhl AM, Cravatt BF.** 2013. NNMT promotes epigenetic remodeling in cancer by creating a metabolic methylation sink. Nat. Chem. Biol. **9:**300–306. http://dx.doi.org/10.1038/nchembio.1204.
51. **Liang G, Zhang Y.** 2013. Embryonic stem cell and induced pluripotent stem cell: an epigenetic perspective. Cell Res. **23:**49–69. http://dx.doi.org/10.1038/cr.2012.175.
52. **Ang Y-S, Tsai S-Y, Lee D-F, Monk J, Su J, Ratnakumar K, Ding J, Ge Y, Darr H, Chang B, Wang J, Rendl M, Bernstein E, Schaniel C, Lemischka IR.** 2011. Wdr5 mediates self-renewal and reprogramming via the embryonic stem cell core transcriptional network. Cell **145:**183–197. http://dx.doi.org/10.1016/j.cell.2011.03.003.